Pertanika J. Sci. & Technol. 33 (2): 653 - 676 (2025)

PERTANIKA JOURNALS

SCIENCE & TECHNOLOGY

Journal homepage: http://www.pertanika.upm.edu.my/

Leveraging Computational Model Approach in Understanding Infectious Disease: A Case Study in Sabah, Malaysia

Siti Sarah Mohd Isnan[1,2], Ahmad Fikri Abdullah[3]*, Abdul Rashid Mohamed Shariff[1], Iskandar Ishak[4], Sharifah Norkhadijah Syed Ismail[5], Doria Tai[6] and Maheshwara Rao Appanan[7]

[1]Faculty of Defence Science and Technology, Universiti Pertahanan Nasional Malaysia, 57000 Kem Sg Besi, Malaysia
[2]Department of Biological and Agricultural Engineering, Faculty of Engineering, University Putra Malaysia, 43400 UPM, Serdang, Selangor, Malaysia
[3]International Institute of Aquaculture and Aquatic Sciences (I-AQUAS), Universiti Putra Malaysia, Port Dickson 70150, Malaysia
[4]Department of Computer Science, Faculty of Computer Science and Information Technology, Universiti Putra Malaysia, 43400 UPM, Serdang, Selangor, Malaysia
[5]Department Environmental and Occupational Health, Faculty of Medicine and Health Sciences, University Putra Malaysia, 43400 UPM, Serdang, Selangor, Malaysia
[6]Sabah State Department, Floor 12-14, Block A, Sabah State Administrative Centre, Jalan Sulaiman, Teluk Likas, 88400 Kota Kinabalu, Sabah, Malaysia
[7]Ministry of Health Malaysia, 62000 Putrajaya, Malaysia

ABSTRACT

The COVID-19 pandemic due to the SARS-CoV-2 coronavirus has vastly impacted our national health and economic industries. Hence, the utilisation of big data simulation of the outbreak is essential to guide policymakers, government, and health authorities in better understanding the dynamics of the infectious disease. This paper integrates the Agent-Based-Model (ABM) and Susceptible, Exposed, Infectious and Recovered (SEIR) framework to understand the dynamic transmission of COVID-19 in Sabah, Malaysia. This study employed NetLogo software, which includes parameters such as geographical distribution, population density, variant type, lockdown measures, and vaccination rates across 27 districts, to run the simulation and assess the potential impact of public health interventions. The methodology involves different scenario simulations using varying variant types, vaccination coverage, lockdown, and social distancing measures to determine the virus transmission level. The results indicate that higher vaccination coverage and strict adherence

ARTICLE INFO

Article history:
Received: 16 April 2024
Accepted: 19 August 2024
Published: 21 February 2025

DOI: https://doi.org/10.47836/pjst.33.2.06

E-mail addresses:
sarahmohdisnan@gmail.com (Siti Sarah Mohd Isnan)
ahmadfikri@upm.edu.my (Ahmad Fikri Abdullah)
rashidpls@upm.edu.my (Abdul Rashid Mohamed Shariff)
iskandar_i@upm.edu.my (Iskandar Ishak)
norkhadijah@upm.edu.my (Sharifah Norkhadijah Syed Ismail)
doria.tai@sabah.gov.my (Doria Tai)
mahesh@moh.gov.my (Maheshwara Rao Appanan)
* Corresponding author

ISSN: 0128-7680
e-ISSN: 2231-8526

to preventive measures can reduce the spread of the virus, especially in highly densely populated areas. Our simulation resulted in a 2.54% variance with the true data following the parameters and settings mentioned above. Additionally, this study also found that geographical structure and uneven distribution of healthcare across the Sabah district notably affect disease and disaster management and intervention policy and efficacy. These insights are crucial for Malaysian policymakers and health authorities, which need to tailor the public health responses considering geographical and demographic settings. Future recommendations include data of higher geographical resolution, immunisation records, and real-time mobility data to portray a more realistic simulation.

Keywords: ABM, big data, COVID-19, epidemiology, infectious disease, SEIR

INTRODUCTION

COVID-19 is caused by Severe Acute Respiratory Syndrome Coronavirus 2, known as SARS-CoV-2, which has affected countries worldwide since March 2020 (López & Rodó, 2021). The first case was reported in December 2019 in Wuhan, China, and it spread all over the world until WHO announced it as a pandemic in March 2020 (Shamil et al., 2021). By June 2023, the number of COVID-19 cases worldwide had exceeded 767 million, and deaths had reached almost 7 million (World Health Organization, 2023b). Governments around the world have implemented various measures to curb the spread of the virus, such as social distancing, travel restrictions, and widespread testing (Shah et al., 2020). Despite these efforts, the number of confirmed cases has continued to rise, and the pandemic has significantly impacted the country's economy, healthcare system and society (Gill et al., 2020). International research to aid policymakers in combatting the virus is crucial to avoid more loss, especially in economic industries (Cheng et al., 2020).

In Malaysia, the first COVID-19 case was reported in January 2020, followed by a total lockdown in March 2020, which has caused catastrophic effects on economic industries and other government and private sectors (Roslan et al., 2022). Sabah, particularly a state in Malaysia, has also experienced the devastating effects of the outbreak. A study by Azzeri et al. (2020) has proven that Sabah communities were experiencing significant health issues even before COVID-19 appeared. M. Goroh et al. (2020) have reported that Sabah is experiencing high cases of infectious diseases such as tuberculosis. Additionally, the Sabah citizens are experiencing difficulties in healthcare facilities and delivery due to the geographical location separating them from the main Peninsular of Malaysia. Tha et al. (2020) mentioned that the geographical features in Sabah, especially in rural areas, have further hindered the healthcare system accessibility there due to the steep hills and rivers.

Patients with COVID-19 have experienced difficulties accessing hospitals and clinics to get treated and get vaccinations (Yeo, 2020). Scholars such as Azhary et al. (2022) have demonstrated that the healthcare services in rural areas of Sabah are 48% lower than in Peninsular Malaysia, which is around 68% in terms of longer travel time and distance

to access healthcare facilities. Due to this, COVID-19 patients may not be able to be treated properly, causing morbidity and mortality rates to be high. As stated by Jafar et al. (2024), the vaccination rate of COVID-19 in Sabah is lower compared to Peninsular Malaysia; therefore, dynamic predictions in the Sabah area will provide valuable insights into determining the epidemiological characteristics, analysing the effects of interventions, and offering useful insights into the dynamics of the disease. They assist policymakers and public health professionals in making decisions about allocating resources and implementing efficient control measures. Among the various models and approaches used to predict the dynamics of COVID-19, the SEIR model is one of the famous methods for studying COVID-19 transmission (Thompson & Wattam, 2021). The SEIR model divides the population into four compartments: susceptible, exposed, infectious, and recovered (Qiu et al., 2022). SEIR model uses dynamic equations to detect the dynamics of COVID-19. Hence, the adaptive numerical method, introduced by Qureshi et al. (2023) and Hassan et al. (2023), is useful for increasing the accuracy of the simulations, especially when dealing with unpredictable and variable changes in COVID-19.

Most researchers incorporated and added new variables in their research. For example, Silva et al. (2020) used the SEIR model to simulate the dynamics of COVID-19 using a society of agents emulating people, businesses, and government in Brazil. Pandey et al. (2019) used the SEIR model and regression analysis to predict the dynamics and patterns of COVID-19, while Avinash et al. (2022) used optimisation to increase the effectiveness of the SEIR model in India. Kucharski et al. (2020) evaluated the effectiveness of isolation, testing, contact tracing, and physical distancing measures with different parameters using the SEIR model in the United Kingdom. Almeshal et al. (2020) and Zhao et al. (2022) combined logistic regression and the SEIR model to predict the COVID-19 cases in China and Kuwait. Paul et al. (2020) compared the effectiveness of the SEIR model in different regions of India and Brazil. Yang et al. (2020) modified the SEIR model by integrating the population variable into the mathematical model in China, while Mwalili et al. (2020) incorporated environment and social distancing in the compartment model in order to increase the efficiency of the model.

Agent-Based Model (ABM) is a model that can be used to better understand the dynamics of infectious disease, as it allows researchers to capture the heterogeneity of the disease by simulating a population of agents with varying characteristics and behaviours (Farheen et al., 2022). ABM also enables researchers to explore different scenarios and interventions to see how they might affect the spread of the disease, such as the effects of social distancing measures or vaccination campaigns (Dong et al., 2022). Additionally, ABM can account for spatial heterogeneity by simulating interactions between agents within geospatial data, which is able to help policymakers and public health officials make informed decisions about how to respond to infectious diseases (Thompson & Wattam, 2021).

Dong et al. (2022) utilised the agent-based model to simulate the COVID-19 cases using geographical data in China. However, Kim and Cho (2022) used the ABM model to investigate the effectiveness of control measures in order to control COVID-19 in a closed environment. Farheen et al. (2022), Hinch et al. (2021), and Shamil et al. (2021) used ABM to simulate the dynamics of COVID-19 in the USA, United Kingdom and Bangladesh. Hunter and Kelleher (2022) also used ABM to simulate the effect of crowdedness in Ireland. Compartmental models are useful for modelling disease transmission mechanisms. However, they require the assumption of complete mixing within compartments and ignore many other factors such as geography, population heterogeneity, individual contact vectors, social dynamics, governmental decisions (e.g., lockdown measures), and other human behaviour complexities (Kong et al., 2022). The COVID-19 pandemic has highlighted the need for accurate and reliable models to understand the spread of infectious diseases and develop effective strategies to control their transmission. While compartmental models such as SEIR have been widely used to study the transmission dynamics of COVID-19, they have several limitations, including the assumption of complete mixing within compartments and the lack of consideration for individual behaviours, population heterogeneity, and other factors that can influence the spread of the virus (Kong et al., 2022).

Hence, to overcome these limitations, scholars have tried to simulate infectious diseases using ABM, which is able to produce results of complex patterns (Dong et al., 2022). By integrating SEIR models with ABMs using big data, researchers can develop more accurate and realistic models to understand the dynamics of infectious disease outbreaks in specific contexts, such as the Malaysian population, with its unique cultural practices and available resources (Tang et al., 2017). As a result, this integration can offer a more thorough and precise understanding of the transmission of infectious illnesses as well as the efficacy of interventional measures. The architecture of the combined SEIR-ABM model involves simulating the behaviour of individual agents and their interactions with each other and their environment. It also incorporates the SEIR model to capture the spread of the disease.

In this context, the paper aims to develop an ABM combined with an SEIR model to better understand the patterns and dynamics of COVID-19 transmission in Sabah, Malaysia, by using big data and incorporating factors such as vaccination coverage, population mobility and the transmission rate which is able to simulate the spread of the virus and explore the impact of interventions such as vaccination and the development of herd immunity. The researcher chose Sabah as the study area due to its unique geographical distribution, which makes it a challenge for the accessibility of the healthcare system; hence, this study is important to yield insights both locally with similar geographical challenges (Balakrishnan et al., 2023; M. Goroh et al., 2020; M. M. D. Goroh et al., 2020; Onyechege et al., 2022; Tan et al., 2021). Figure 1 depicts the summary of the SEIR-ABM simulation.

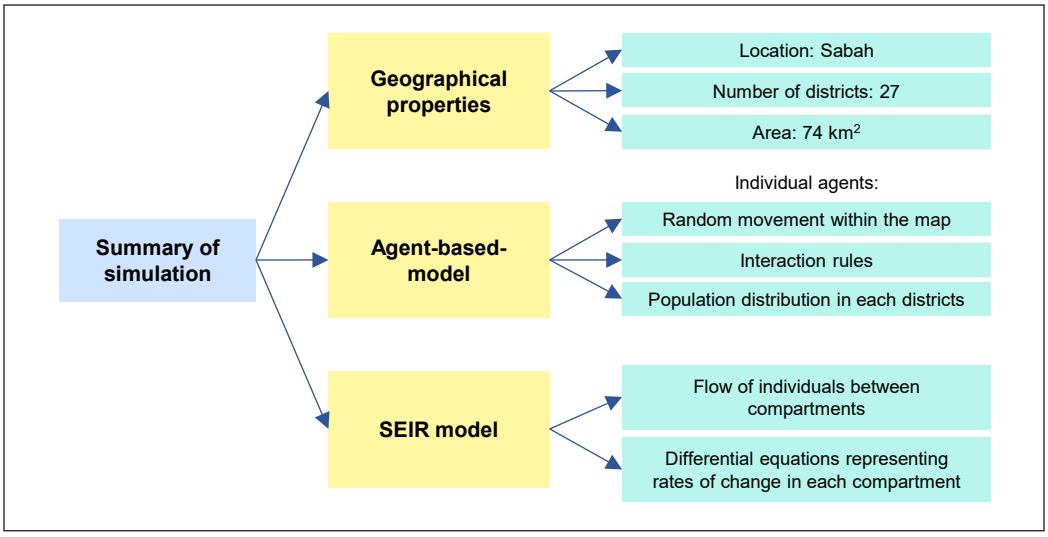

Figure 1. Summary of SEIR-ABM simulation

METHODS

This study focuses on Sabah, a state in Malaysia with a total area of 73, 904 km^2 (M. M. D. Goroh et al., 2020). Sabah has 27 districts, which are Tawau, Papar, Lahad Datu, Tuaran, Putatan, Sipitang, Beaufort, Kota Belud, Kinabatangan, Kunak, Sandakan, Semporna, Ranau, Penampang, Tambunan, Keningau, Labuk Sugut, Kota Marudu, Pitas, Pensiangan, Kudat, Tongod, Telupid, Kuala Penyu, Tenom, Kalabakan and Kota Kinabalu as the capital city of Sabah, each population for each district is depicted as shown in Figure 2 (Azzeri et al., 2020). The average annual temperature of Sabah is around 24°C, which shows the humidity and tropical weather of Sabah throughout the year (Iderus et al., 2022). The annual rainfall is about 2102 mm yearly (Iderus et al., 2022). The geographical feature of Sabah is mostly covered with mountains and tropical rainforests with an altitude range of 4100m (Iderus et al., 2022). Kota Kinabalu, which is the capital of the Sabah, has gone through rapid urbanisation compared to other districts. The data acquisition resources for each variable are shown in Table 1.

Our dataset of 365,115 COVID-19-positive cases was extracted from the Sabah State Government. The dataset was derived from hospital reports in Sabah and sent to the Sabah State Government (Hashim et al., 2021). This data also included the collection of MySejahtera records, which is a mobile application developed by the Malaysian Government to monitor COVID-19 in Malaysia (https://mysejahtera.moh.gov.my/ms/). The data contains the district-level cases, confirmed cases, recovered cases, and death cases. Our population demographic data was obtained from the Department of Statistics, Malaysia, during the 2020 census. This data acts as a true representation of the population

in each district of Sabah. The data collection period covered the period of the outbreak from March 2020 until March 2022.

The attributes dataset, which includes rivers, buildings, mountains, forests, and roads, is downloaded from the Open Street Map website (Relation: Malaysia (2108121) | OpenStreetMap). After that, the Sabah district, rivers, roads, buildings, and mountains are imported into ArcMap 10.8 for checking. All these layers are aligned with each other using the Projected Coordinates of WGS 1984. The map of the Sabah in ArcMap is shown in

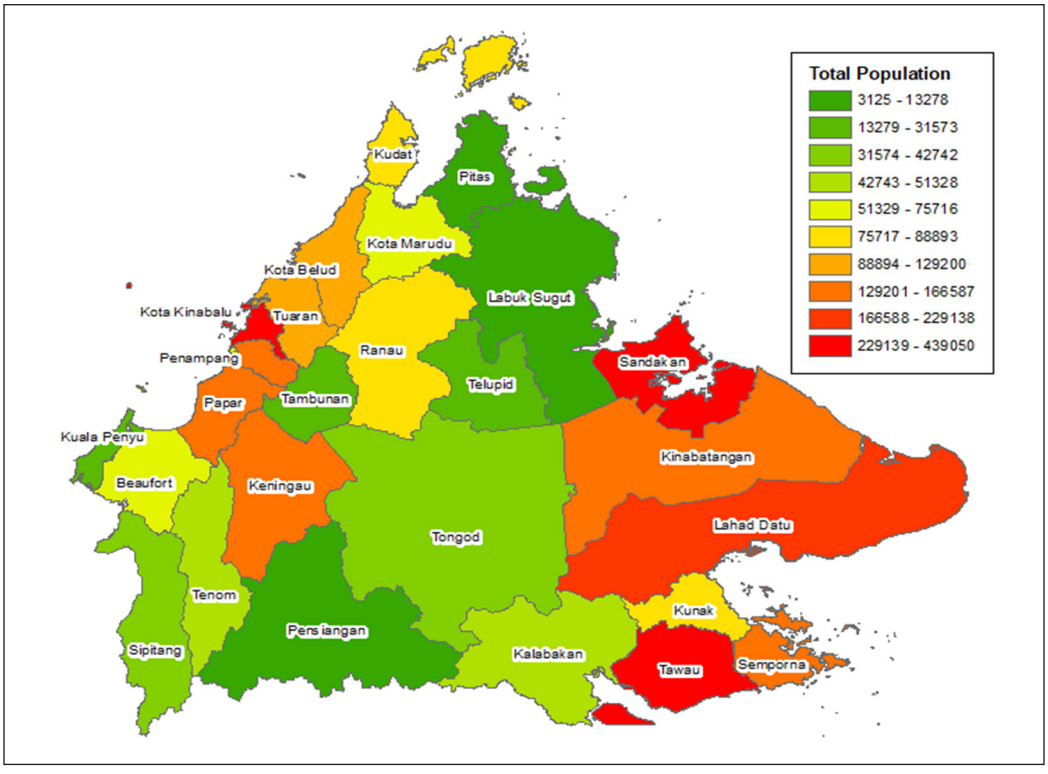

Figure 2. Map of Sabah districts and their total number of populations

Table 1
Data acquisition resources

Data	Source	Period/Year
District of Sabah Shapefile	Sabah State Government	2020
Buildings	Open Street Map	2020
Roads		2020
Mountains and Forest		2020
Rivers		2020
Number of populations by district in Sabah	Department of Statistics Sabah	Census data for the year 2020

Figures 3 and 4. We separated the geographical features into two different maps for better visualisation, as distinguishing different geographical features on a large map of Sabah is challenging due to the large scale of the Sabah area. However, a large number of attributes have caused ArcMap 10.8 to perform slower when loading various elements.

The simulation of the outbreak is performed in the NetLogo Software Version 6.4.0. All the geographical layers are imported in NetLogo, as shown in the code of Figure 5. As for this model, the agent or turtle is a person in every district of Sabah. The total number of people in each district depicted the total population. The researcher set the location and movement of each person at random, as this study does not exhibit the location and mobility data of each positive COVID-19 case. Hence, the assumptions of the models are:

1. Number of populations remains constant based on the data.
2. Random movement at rate 2.0 within the map.
3. Recovered people become immune; if they have already been infected and recovered, they will not be infected for the second time.

The SEIR model can be represented graphically using a set of differential equations (Equations 1 to 4), which describe the flow of individuals between compartments over time (https://docs.idmod.org/projects/emod-hiv/en/2.20_a/model-seir.html).

$$\frac{dS}{dt} = -\frac{\beta IS}{N} \qquad [1]$$

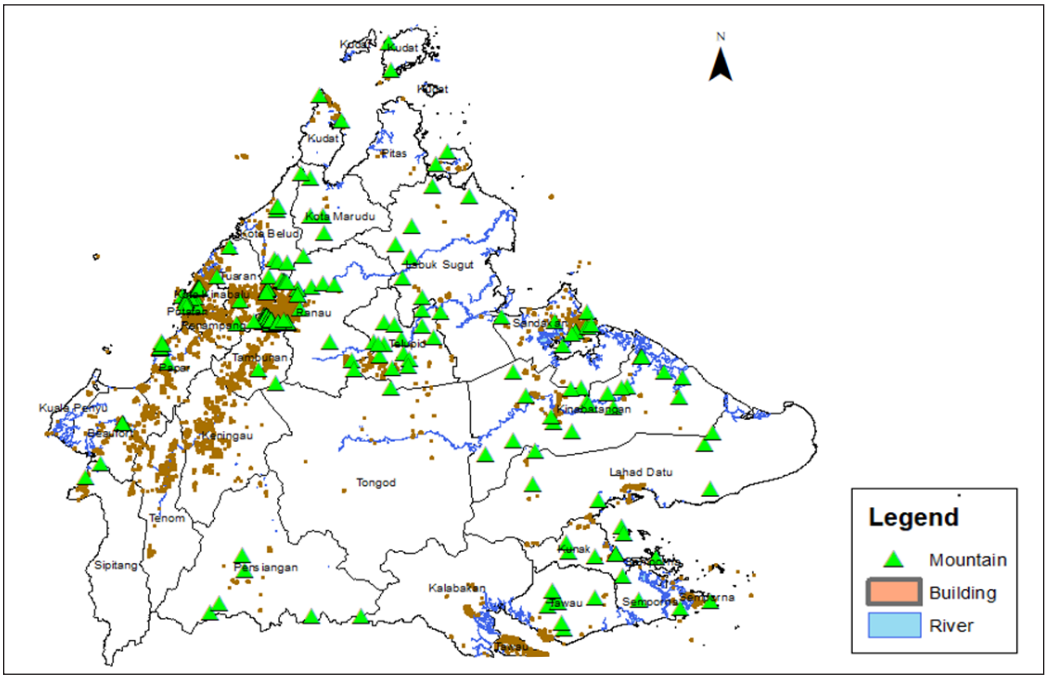

Figure 3. Distribution of buildings, rivers and mountains in Sabah

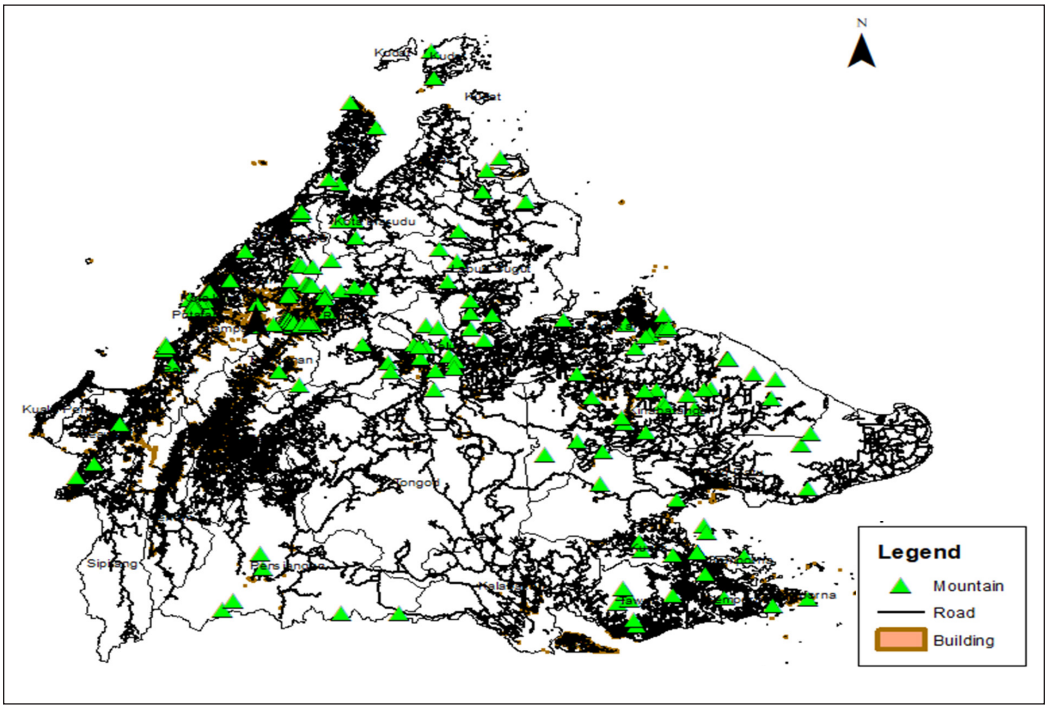

Figure 4. Distribution of roads, rivers and mountains in Sabah

$$\frac{dE}{dt} = -\frac{\beta IS}{N} - \sigma E \quad [2]$$

$$\frac{dI}{dt} = \sigma E - \gamma I \quad [3]$$

$$\frac{dR}{dt} = \gamma I \quad [4]$$

Where: dS/dt = the change in the number of susceptible individuals over time; dE/dt = the change in the number of exposed individuals over time; dI/dt= the change in the number of infectious individuals over time; dR/dt = the change in the number of recovered individuals over time; ß = the disease transmission rate from infectious individuals to susceptible individuals; σ = the rate at which exposed individuals become infectious; γ = the rate at which infectious individuals recover or develop immunity.

Based on Equation 1, it depicted the rate of change of the susceptible over time. The total number of susceptible people is inversely proportional to the number of infected people; hence, it is indicated by the negative sign (He et al., 2020). The rate of change is directly proportional to the rate of transmission (β), the number of infected persons (I) and the remaining susceptible persons (S/N) (He et al., 2020). Equation 2 depicts the rate

of change of the exposed people over time. The negative sign indicated that the number of exposed people is inversely proportional over time as by the time they will recover and become infectious (He et al., 2020). The rate of change is directly proportional to the same state as the susceptible conditions and the rate at which the exposed persons become infectious (σ) (He et al., 2020). Equation 3 shows the rate of change of the infected persons over time. The rate at which people move from the exposed condition to the infected condition is represented by positive signs. However, the negative sign is represented by the rate at which people recover and move to the recovered condition (He et al., 2020). Equation 4 depicts the rate of change of recovered people over time, which shows the infected people recovered and moved to the recovered compartment represented by the positive sign (He et al., 2020).

The simulation started by creating a population of citizens, each with its characteristics, such as days after exposure and days of sickness. After that, the simulation will run a series of procedures to mimic the virus's spread among them. The simulation is divided into procedures, each of which simulates a distinct element of the outbreak. The setup process starts the simulation by loading a GIS shapefile and creating citizens within the shapefile's area. The population-list variable, which contains a list of population sizes for each district, determines the total number of citizens created in each district.

Each citizen is chosen at random to be infected with the virus. The go procedure is the simulation's primary loop. It begins by determining whether the simulation has ended, with all residents recovering or dying. If not, it performs the following procedures:

1. The moving procedure mimics citizen mobility by randomly rotating and moving citizens forward, with a check to see if the target patch is a valid path.
2. The transmission process mimics the virus spread among citizens, with carriers (citizens with the orange colour) spreading the virus to susceptible citizens within a 1-patch radius, as social distancing lower than 1 metre will increase the risk of infection (Badr et al., 2020).
3. The incubation process mimics the virus's incubation period, with carriers becoming infectious after a certain number of days (determined by the incubation period variable) and turning red. In the case of this simulation, we chose 6 days as the incubation period following a recommendation by the World Health Organisation (World Health Organization, 2023a)
4. The sickness process mimics the virus's period, with infectious citizens recovering or dying after a set number of days (determined by the mortality and recovery rates). The transmission rate is set at 75 and 100 to compare the effect of these two conditions and the mortality rate at 10.
5. The find-max-daily-cases procedure keeps track of the simulation's highest number of daily cases.

6. The mobility procedure keeps the movement of the citizens throughout the districts. The movement is set to 0.5 and 1.0 to compare the results.
7. Other processes in the simulation include vaccinating, which simulates vaccination by randomly selecting a certain proportion of susceptible citizens and changing their colour to blue to symbolise immunity.
8. A watch-an-infected-person process also highlights a randomly selected infected citizen for visualisation reasons.
9. The variant type provides how fast the COVID-19 virus spreads to another person. For example, the Omicron and Delta variants have a higher transmission rate.
10. The transmission rate indicates the speed of the transmission, which is denoted by the type of variant. A transmission rate of 80 for Omicron, 70 for Delta, and 40 for Alpha denotes a higher susceptibility of the variant (Umair, 2022).
11. The mountains, buildings, roads and rivers act as geographical features that allow the person to move more realistically. Roads facilitate faster transmission; however, mountains and rivers can be denoted as obstacles that limit movement and slow down the spread of the virus.

```
to setup
  clear-all
  set scale 30
  set population-list [75716 48195 150927 143112 107243 371221 69528 23710 86410 88893 3125
                       13278 3666 68811 85077 439050 166587 37828 31573 372615 29241 51328
  set country gis:load-dataset "C:/Sabah_District_Boundary/district_no_sea.shp"
  set rivers gis:load-dataset "C:/Shp/River/River.shp"
  set roads gis:load-dataset "C:/Shp/Road/Road.shp"
  set mountForest gis:load-dataset "C:/Shp/Mountain/Mountain.shp"
  set building gis:load-dataset "C:/Shp/Building/Building.shp"
  gis:set-world-envelope (gis:envelope-union-of (gis:envelope-of country)
                                                (gis:envelope-of rivers)
                                                (gis:envelope-of roads)
                                                (gis:envelope-of mountForest)
                                                (gis:envelope-of building))
  display-country
  if river? [draw-rivers]
  if road? [draw-roads]
  if building? [draw-building]
  if mountain? [draw-mountForest]
  create-paths
  create-citizens-in-country
  set susceptible count citizens with [color = yellow]
  ;show susceptible
  ;show count citizens
  set died-citizen 0
  set watching false
  reset-ticks
end

;-----------------------------------------------------------------------

to display-country
  gis:set-drawing-color brown
  gis:draw country 1
end
```

Figure 5. Script to load geographical layers in Netlogo 6.4.0

12. The lockdown rate parameter also restricts mobility to reduce the spread of the virus (Dong et al., 2022).
13. Social distancing also indicates virus spread mitigation (López & Rodó, 2021).

RESULTS

The model begins with a human population comprised of susceptible (yellow-coloured) individuals, as in Figure 6. When a person exposed to the disease (orange colour) enters the community, he or she will spread the disease to one of the susceptible people nearby (within a radius of less than 1 metre) at the stated transmission rate as in Figure 7. After the specified incubation period, the exposed may develop ill (infectious red colour), as shown in Figures 8 and 9. The sick will be quarantined so that they do not infect others. The sick individuals will be hospitalised for 14 days. They either die (disappear from the model) on the 15th day of illness or recover and become immune to the sickness (blue colour), as in Figures 10 and 11. Each citizen is allocated a sex, colour, and size, with some being chosen at random to be disease carriers (orange colour). Citizens travel across the nation randomly, with mobility limited by areas of green pavement. The model also incorporates a vaccine mechanism that vaccinates citizens at random with a predetermined probability. The simulation is performed on a grid, with each cell representing a district in the region, and citizens are assigned to each cell based on the district's population density. The simulation terminates when there are no more citizens with the red colour, i.e., contagious citizens. During the simulation, the model maintains track of the number of residents who died as a result of the virus, together with the maximum number of daily cases.

The mobility movement is set to random as this study does not exhibit mobility data. More simulations will produce more accurate results because of the nature of the random

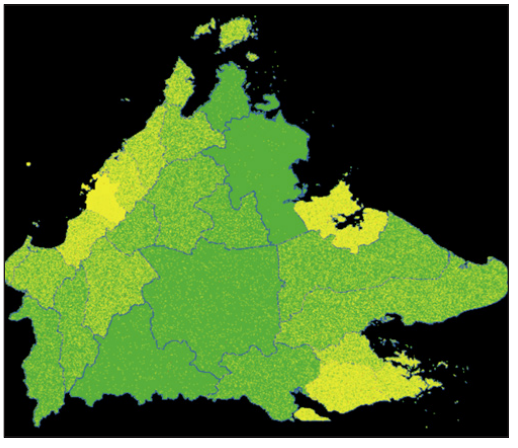

Figure 6. Susceptible person in yellow colour on day 1 during simulation one

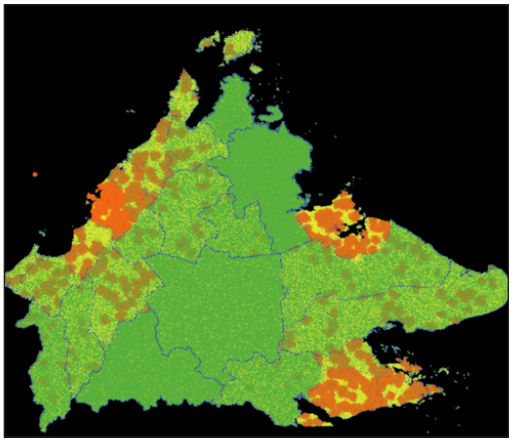

Figure 7. Exposed person in orange colour day 10 during simulation one

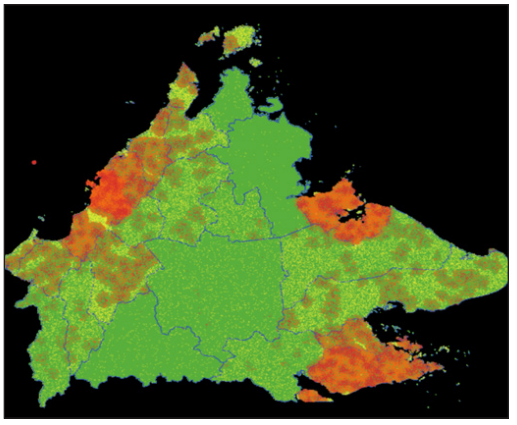

Figure 8. Infected person in red colour day 20 during simulation one

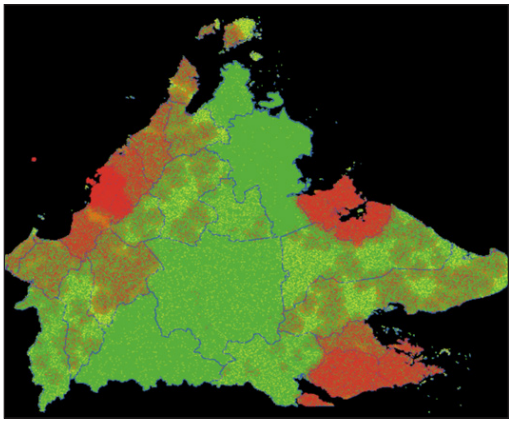

Figure 9. Simulation of Sabah map showing increasing of infected persons day 23 during simulation one

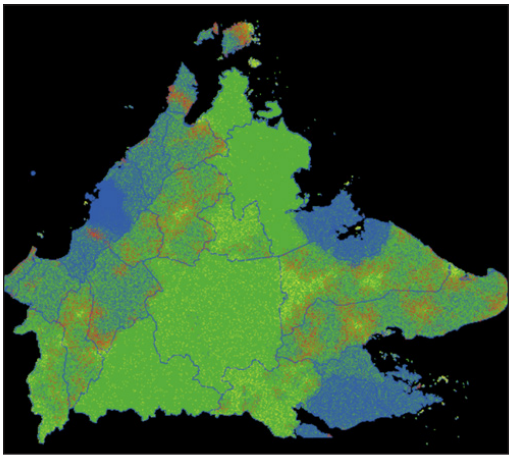

Figure 10. Recovered/vaccinated person in blue colour day 190 during simulation 1

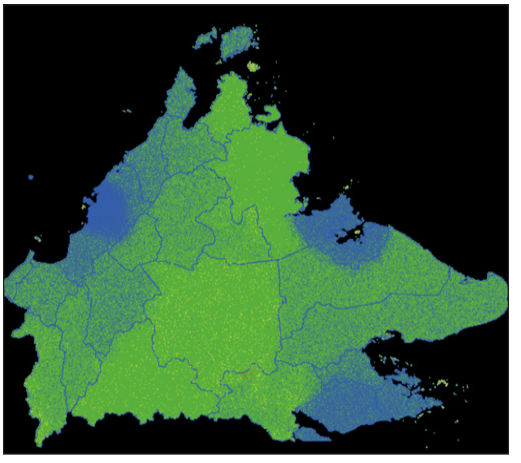

Figure 11. Sabah map showing infected person that has recovered day 210 during simulation one

movement (Motzev, 2019). Since the movement of the agent is set to random, the agent may sometimes move in a direction that is not optimal or may even move in the opposite direction of the target. In other words, running multiple simulations helps reduce the effect of randomness in the agent's movements, leading to more accurate and reliable results. By averaging the results from multiple simulations, the researcher can get a more representative sample of the agent's performance and reduce the impact of individual instances of suboptimal or random movements.

Fifteen simulations were run with the parameters in Table 2 to investigate the impact of different combinations of parameters on the spread of the disease. The simulations were designed to test the effectiveness of various interventions, such as vaccination rates, transmission rates, incubation periods, mobility, social distancing, lockdown, and

Table 2
Parameters setting for 15 simulations

Simulation	The initial number of infected cases	Vaccination rate	Transmission Rate	Mortality	Incubation Period	Mobility	Type of variant	Lockdown	Social Distancing
1	8	78	75	10	6	0.5	-	-	-
2	8	78	75	10	6	1	-	-	-
3	8	78	100	10	6	0.5	-	-	-
4	8	78	100	10	6	1	-	-	-
5	20	100	50	10	6	1	-	-	-
6	20	100	100	10	6	1	-	-	-
7	20	0	50	10	6	1	-	-	-
8	20	0	100	10	6	1	-	-	-
9	20	100	50	10	6	1	-	-	-
10	20	100	100	10	6	1	-	-	-
11	200	0	70	10	6	0.5	Delta	Yes	Yes
12	200	0	70	10	6	0.5	Delta	No	No
13	8	78	75	10	6	0.5	Delta	Yes	Yes
14	200	45	80	10	6	1	Omicron	Yes	Yes
15	200	60	80	10	6	1	Omicron	No	Yes

variant types, in controlling the spread of the disease. The simulations were conducted to gain a better understanding of the complex interactions between these variables and to make more informed decisions about how to control the spread of the disease (Kim & Cho, 2022; Gharakhanlou & Hooshangi, 2020; Nagori et al., 2020). Figure 12 shows the NetLogo interface to run the simulation, as stated in Table 1. All settings are stated in the methodology section. Figure 13 depicts the screenshot of the NetLogo 6.4 scripts to load geographical features of rivers, roads, mountains and buildings.

Figure 14 shows the Graph of Simulation One with a transmission rate of 75, mortality of 10, incubation period of 6 days and mobility rate of 0.5. Based on the graph, the number of infected cases reached around 1.60 million within 25 days, recovered cases reached around 2.5 million within 143 days and died cases of 293,640 cases within 199 days. This simulation took around 210 days for all the infected cases to be recovered, and no more infections were transmitted.

Simulation Two demonstrated a transmission rate of 75, mortality of 10, incubation period of 6 days and mobility rate of 1. Based on the results, infected cases reached 2.05 million within 23 days, recovered cases reached around 2.71 million within 143 days and died cases of 300,480 cases within 130 days. This simulation took around 143 days for all the infected cases to be recovered, and no more infections were transmitted.

Simulation Three demonstrated a transmission rate of 100, mortality of 10, incubation period of 6 days and mobility rate of 0.5. Based on the results, the infected cases reached around 1.76 million within 23 days, recovered cases reached around 2.65 million within

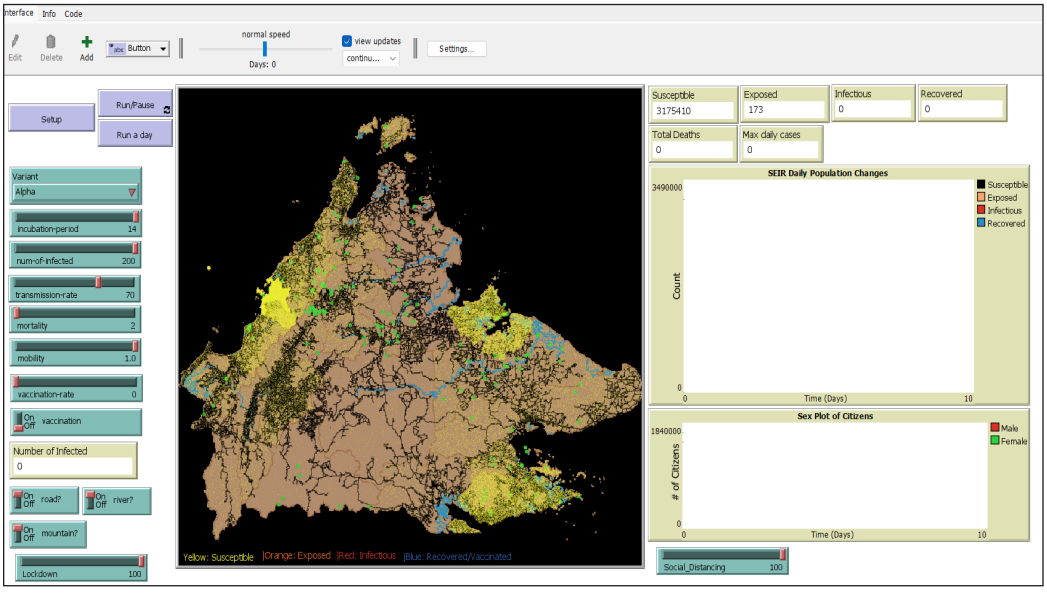

Figure 12. Table 1 lists the NetLogo interface to run the simulation. The methodology section states all settings

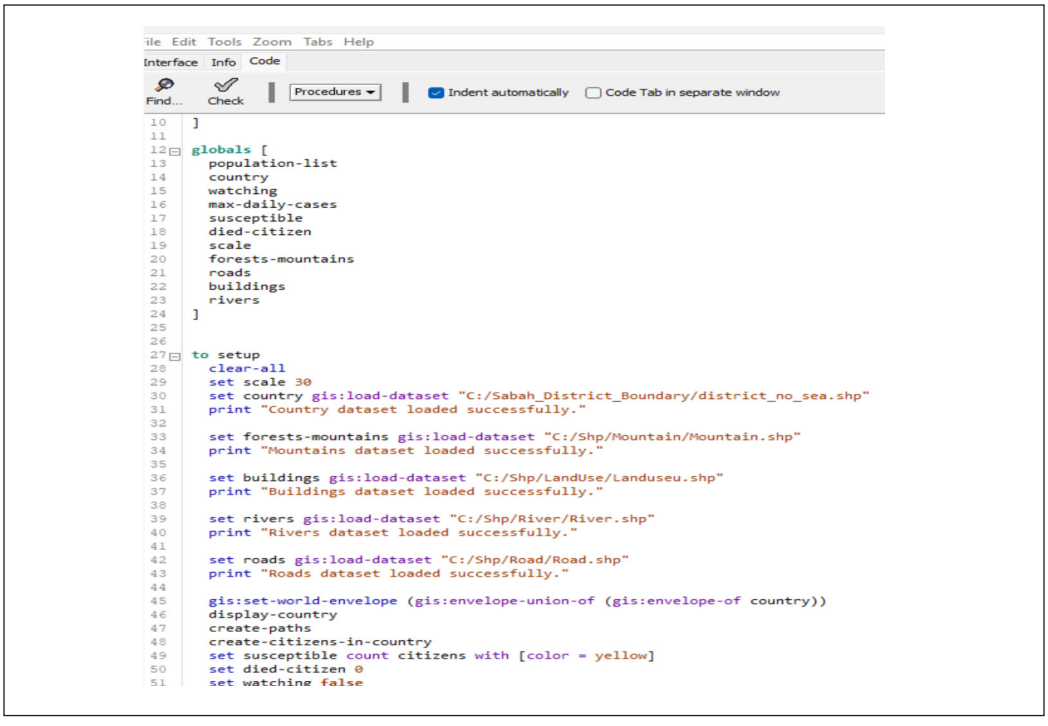

Figure 13. Screenshot of the NetLogo 6.4 scripts to load geographical features of rivers, roads, mountains and buildings

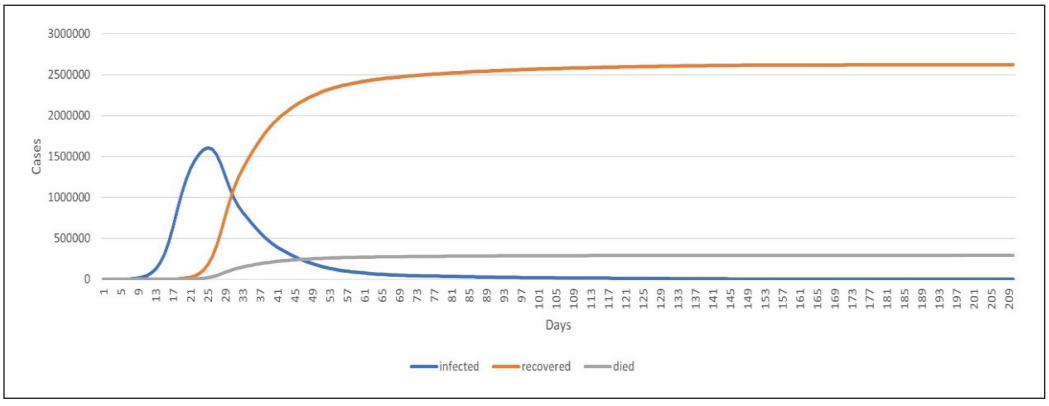

Figure 14. Graph of simulation one

211 days and dead cases 292,740 within 212 days. This simulation took around 212 days for all the infected cases to be recovered.

Simulation Four tested a transmission rate of 100, mortality of 10, incubation period of 6 days and mobility rate of 1. Based on the results, the graph of infected cases reached around 2.07 million within 23 days, recovered cases reached around 2.73 million within

207 days and died cases 292,740 within 207 days. This simulation took around 207 days for all the infected cases to be recovered.

Simulation Five demonstrated a transmission rate of 50, mortality of 10, incubation period of 6 days, vaccination rate of 100%, initial number of infected cases of 20 and mobility rate of 1. Based on the results, the infected cases reached around 14,400 within 8 days, recovered cases reached around 3.17 million within 19 days and died cases 1,620 within 19 days. This simulation took around 19 days for all the infected cases to be recovered.

Simulation Six tested a transmission rate of 100, a mortality of 10, an incubation period of 6 days, a vaccination rate of 100%, an initial number of infected cases of 20 and a mobility rate of 1. Based on the results, the infected cases reached around 15,300 within 7 days, recovered cases reached around 3.17 million within 19 days and died cases 1,620 within 19 days. This simulation took around 19 days for all the infected cases to be recovered.

Simulation Seven demonstrated a transmission rate of 50, a mortality of 10, an incubation period of 6 days, a vaccination rate of 0%, an initial number of infected cases of 20 and a mobility rate of 1. Based on the results, the infected cases reached around 21,450 within 7 days, recovered cases reached around 2.67 million within 161 days and died cases 294,900 within 161 days. This simulation took around 161 days for all the infected cases to be recovered.

Simulation Eight demonstrated a transmission rate of 100, a mortality of 10, an incubation period of 6 days, a vaccination rate of 0%, an initial number of infected cases of 20 and a mobility rate of 1. Based on the results, the infected cases reached around 28,560 within 8 days, recovered cases reached around 2.76 million within 143 days and died cases 303,330 within 143 days. This simulation took around 161 days for all the infected cases to be recovered.

Simulation Nine tested a transmission rate of 50, a mortality of 10, an incubation period of 6 days, a vaccination rate of 100%, an initial number of infected cases of 20 and a mobility rate of 1. Based on the results, the infected cases reached around 23,520 within 8 days, recovered cases reached around 3.17 million within 23 days and died cases 2880 within 23 days. This simulation took around 23 days for all the infected cases to be recovered.

Simulation Ten tested a transmission rate of 100, a mortality rate of 10, an incubation period of 6 days, a vaccination rate of 100%, an initial number of infected cases of 20 and a mobility rate of 1. Based on the results, the infected cases reached around 26,430 within 8 days, recovered cases reached around 3.17 million within 23 days and died cases reached 4,350 within 23 days. This simulation took around 23 days for all the infected cases to be recovered.

Simulation 11 demonstrated a transmission rate of 70, the Delta variant with 200 initial infected cases, no vaccination with a mobility rate of 0.5, and the implementation of lockdown and social distancing. Based on the results, the infected cases reached around 1,003 within 28 days, recovered cases reached around 973 within 200 days, and death cases reached around 30 within 40 days. The simulation took 200 days to complete.

Simulation 12 performed the same parameters as Simulation 11 but without lockdown and social distancing. The results of the initial infected cases are higher: 5,73 cases within 21 days, 5,625 recovered cases within 31 days and 48 death cases within 31 days. This simulation took 212 days to complete.

Simulation 13 demonstrated the same parameters as Simulation 1, with the added parameters of Delta variant, social distancing and lockdown, and an initial infected number of 8 cases. The results show that the number of infected cases is smaller than those in Simulation 1, which included 127 cases, 112 recovered cases, and six death cases within 197 days.

Simulation 14 demonstrated 200 initial infected cases with the Omicron variant at a 45% vaccination rate and an 80% transmission rate. The results showed that the infected cases became 5495, recovered 5148, and death cases 20 within 183 days consecutively.

The final simulation demonstrated a higher vaccination rate of 60% without lockdown intervention. The infected cases became 4193, the recovered cases 4441 and 17 deaths occurred within 171 days. Hence, Table 3 summarises the simulation results.

Table 3
Simulation results

Simulation	Infected cases	Day	Recovered cases	Day	Died Cases	Day	Days to complete
1	160	25	2,622,750	210	293,640	199	210
2	205	24	2,713,320	143	300,480	130	143
3	176	23	2,656,890	211	292,740	212	212
4	207	23	2,730,780	207	300,270	185	207
5	14,400	8	3178980	19	1620	19	19
6	15,030	8	3178980	19	1620	19	19
7	1994730	26	2665800	161	294900	147	161
8	2454750	21	2764920	143	303330	128	143
9	31560	12	3177690	23	2880	22	23
10	42330	12	3176220	23	4350	22	23
11	1003	28	973	200	30	40	200
12	5673	21	5625	212	48	31	212
13	127	19	112	197	6	27	197
14	5495	22	5148	183	20	28	183
15	4192	18	4441	171	17	19	171

DISCUSSION

The different parameters and interventions simulated using NetLogo provide dynamics transmission results in the case of COVID-19. Throughout this study, parameters such as vaccination rate, transmission rate, the initial number of infected cases, incubation period, mobility rate, social distancing, lockdown intervention, and geographical features play an important role in depicting the real-world situation, which highlights the nuanced interplay of these factors in disease outbreak management.

The initial number of infected cases proves to be one factor that leads to a higher number of cases, such as in Simulations 5 and 8. The higher the number of infected cases, the higher the susceptibility of the citizens to be exposed to the infected, causing the number of cases to spike faster (Balakrishnan et al., 2023). The higher vaccination rate, such as in Simulation 10, is effective in curbing the disease spread, which shows that the vaccination program is effective in controlling the severity effect of the infectious disease (Chen et al., 2022). The types of variants, especially Omicron and Delta, with higher transmission rates demonstrated that these variants are contagious and a higher vaccination rate is able to reduce mortality and higher mobility produced higher cases, especially in the absence of movement restrictions (lockdown) and social distancing rate (Chenchula et al., 2022).

The first case in Sabah was reported on 25 January 2020, but Sabah remained unaffected by this case until Sri Petaling tabligh cases appeared, which caused a massive wave in Malaysia, including Sabah (Balakrishnan et al., 2023). We compared the simulated cases with the real-world cases that occurred in Sabah from March 2020 until March 2022. Simulation 1 to Simulation 10 produced a high variance due to the discrepancies with the real-world conditions. However, simulation 11 until simulation 15, which considered the geographical features and obstacles, variant types, social distance, citing and lockdown measures, produced more robust and reliable results with the real-world data for infected and recovered. Simulations 12 and 14 depicted the least variation, about less than 10%, for recovered and infected cases compared to other simulations. However, the simulation of death cases is not successfully captured by the simulation due to the model representing different health states, and it handled the transition between each compartment (susceptible, carrier, infected and recovered) in deterministic modelling (Godio et al., 2020). Data such as different age groups is crucial to determine the death susceptibility as the older age groups may have more severe effects towards the outbreak (He et al., 2020). This comparative analysis demonstrated that simulations 12 and 14 are the most accurate and aligned with the true data in Sabah because the simulation added new parameters such as geographical obstacles, variant types, social distancing and lockdown intervention. The first simulation until simulation 10 shows a large variance with the true data due to significant real-world representation differences, especially in terms of variant differences and geographical features.

The infected cases in Sabah have spiked during August 2021 and February 2022. The emergence of the Delta variant and Omicron in Sabah has caused the number of infected cases to be high, especially without the lockdown intervention. The Delta variant, which arrived in Sabah in June 2021 has caused the COVID-19 cases to spike in August 2021 (3487 cases) (Balakrishnan et al., 2023), which is the same as our predicted cases, around 4192 (20% variance) cases in Simulation 15. The variance is most likely due to a lack of demographic data such as age, severity of the cases and distance of the patient to the nearest health facility (Jiee et al., 2021). Sabah Health Authority Department has taken the initiative to expedite the targeted groups in Sabah, especially those who live in rural areas, to take the vaccination dose to shrink the number of infected COVID-19 cases (Harizah, 2021). This condition is correlated with the study by Dollah et al. (2022), which highlighted that misinformation and information management have impacted youth vaccine hesitancy in Sabah. Moreover, the geographical features in Sabah have shown difficulties for the health authority in accessing and facilitating the distribution of vaccination programmes.

Due to the failure of the vaccination program in Sabah, it only reached less than 50% of the vaccination adult program during the end of 2021; the cases of COVID-19 reached their peak in January 2022 and reached 5565 cases due to the Omicron variant (Balakrishnan et al., 2023; Patrick, 2022). The Omicron variant has a higher transmission rate compared to the Delta variant due to its multiple mutation characteristics in the spike protein of the virus (Reeves et al., 2022). It increases the ability of this variant to bind with human cells and attack the human immune system (Ahasan et al., 2022). Our simulated data in Simulation 12 and 14 are almost identical to the third wave of COVID-19 during the Omicron spread in Sabah. The variance of the prediction with the true data is 2.54% for Simulation 14 and 5.86% for Simulation 12, which makes Simulation 14 more accurate to the actual number of cases. The recovered and death cases during the peak wave are 1708 and 14, respectively. Our prediction estimated around 183 recovered cases and 28 cases, respectively, which was underestimated due to insufficient demographic data.

The limitations of this study are that the simulation assumes a random movement pattern, linear mobility pattern, homogenous population and vaccination rates, which may not accurately reflect real-world mobility patterns. Additionally, Netlogo software is unstable if the dataset is too large, causing the map's performance and visualisation to become very slow to load. Hence, AnyLogic software can be used to overcome this problem.

CONCLUSION

Overall, the simulation is a deterministic and fundamental model that can provide important insights to the local health authority and government by developing an Agent-Based Model integrated with the SEIR model in areas with complex geography.

Simulation with geographical features, lockdown intervention, social distancing, variant types, and vaccine programmes have shown accurate results with a 2.54% variance from the true data. This model can be further tuned with the smaller scale of the granularity of geographical units, social isolation, immunisations and demographic variations. The findings highlight the necessity for efficient preventative strategies, early intervention, and precise statistics to support policy development.

ACKNOWLEDGEMENT

The authors acknowledged University Putra Malaysia for funding this project under IPS Grant Number 9738200.

REFERENCES

Ahasan, R., Alam, M. S., Chakraborty, T., & Hossain, M. M. (2022). Applications of GIS and geospatial analyses in COVID-19 research: A systematic review. *F1000Research*, *9*, 1–18. https://doi.org/10.12688/f1000research.27544.2

Almeshal, A. M., Almazrouee, A. I., Alenizi, M. R., & Alhajeri, S. N. (2020). Forecasting the spread of COVID-19 in Kuwait using compartmental and logistic regression models. *Applied Sciences,* 10(10), Article 3402. https://doi.org/10.3390/app10103402

Avinash, N., Xavier, G. B. A., Alsinai, A., Ahmed, H., Sherine, V. R., & Chellamani, P. (2022). Dynamics of COVID-19 using SEIQR epidemic model. *Journal of Mathematics, 2022*(1), Article 2138165. https://doi.org/10.1155/2022/2138165

Azhary, J. M. K., Leng, L. K., Razali, N., Sulaiman, S., Wahab, A. V. A., Adlan, A. S. A., & Hassan, J. (2022). The prevalence of menstrual disorders and premenstrual syndrome among adolescent girls living in North Borneo, Malaysia: a questionnaire-based study. *BMC Women's Health*, *22*(1), 1–9. https://doi.org/10.1186/s12905-022-01929-1

Azzeri, A., Goh, H. C., Jaafar, H., Mohd Noor, M. I., Razi, N. A., Then, A. Y., Suhaimi, J., Kari, F., & Dahlui, M. (2020). A review of published literature regarding health issues of coastal communities in Sabah, Malaysia. *International Journal of Environmental Research and Public Health, 17*(5), Article 1533. https://doi.org/10.3390/ijerph17051533

Badr, H. S., Du, H., Marshall, M., Dong, E., Squire, M. M., & Gardner, L. M. (2020). Association between mobility patterns and COVID-19 transmission in the USA: A mathematical modelling study. *The Lancet Infectious Diseases*, *20*(11), 1247–1254. https://doi.org/10.1016/S1473-3099(20)30553-3

Balakrishnan, K. N., Yew, C. W., Chong, E. T. J., Daim, S., Mohamad, N. E., Rodrigues, K., & Lee, P. C. (2023). Timeline of SARS-CoV-2 transmission in Sabah, Malaysia: Tracking the molecular evolution. *Pathogens*, *12*(8), 1–17. https://doi.org/10.3390/pathogens12081047

Chen, X., Huang, H., Ju, J., Sun, R., & Zhang, J. (2022). Impact of vaccination on the COVID-19 pandemic in U.S. states. *Scientific Reports*, *12*(1), 1–10. https://doi.org/10.1038/s41598-022-05498-z

Chenchula, S., Karunakaran, P., Sharma, S., & Chavan, M. (2022). Current evidence on efficacy of COVID-19 booster dose vaccination against the Omicron variant: A systematic review. *Journal of Medical Virology*, *94*(7), 2969–2976. https://doi.org/10.1002/jmv.27697

Cheng, X., Han, Z., Abba, B., & Wang, H. (2020). Regional infectious risk prediction of COVID-19 based on geo-spatial data. *PeerJ*, *8*, 1–24. https://doi.org/10.7717/peerj.10139

Dollah, R., Jafar, A., Joko, E. P., Sakke, N., Mapa, M. T., Atang, C., Hung, C. V., & George, F. (2022). Perception of youth in East Malaysia (Sabah) towards the Malaysia national COVID-19 immunisation programme (PICK). *Journal of Public Health and Development*, *20*(1), 203–217. https://doi.org/10.55131/jphd/2022/200116

Dong, T., Dong, W., & Xu, Q. (2022). Agent simulation model of COVID-19 epidemic agent-based on GIS: A case study of Huangpu District, Shanghai. *International Journal of Environmental Research and Public Health*, *19*(16), Article 10242. https://doi.org/10.3390/ijerph191610242

Farheen, F., Shamil, M. S., Rahman Jony, S. S., Ahmad, Z., Sojib, K. H., Chowdhury, A., Niaz Arifin, S. M., Sania, A., & Rahman, M. S. (2022). *An agent-based model for COVID-19 in Bangladesh*. MedRxiv. https://doi.org/10.1101/2022.07.24.22277974

Gill, B. S., Jayaraj, V. J., Singh, S., Ghazali, S. M., Cheong, Y. L., Iderus, N. H. M., Sundram, B. M., Aris, T., Ibrahim, H. M., Hong, B. H., & Labadin, J. (2020). Modelling the effectiveness of epidemic control measures in preventing the transmis. *International Journal of Environmental Research and Public Health*, *17*(15), 1–13. https://doi.org/10.3390/ijerph17155509

Goroh, M. M. D., Rajahram, G. S., Avoi, R., Van Den Boogaard, C. H., William, T., Ralph, A. P., & Lowbridge, C. (2020). Epidemiology of tuberculosis in Sabah, Malaysia, 2012–2018. *Infectious Diseases of Poverty, 9*, 1-11. https://doi.org/10.1186/s40249-020-00739-7

Goroh, M., Rajahram, G., Avoi, R., Cvd, B., William, T., Ralph, A. P., & Lowbridge, C. (2020). *An Epidemiological Review of Tuberculosis in Sabah, Malaysia, 2012-2018*. Research Square. https://doi.org/10.21203/rs.3.rs-28071/v1

Godio, A., Pace, F., & Vergnano, A. (2020). SEIR Modeling of the Italian Epidemic of SARS-CoV-2 Using Computational Swarm Intelligence. *International Journal of Environmental Research and Public Health, 17*(10), Article 3535. https://doi.org/10.3390/ijerph17103535

Gharakhanlou, N. M., & Hooshangi, N. (2020). Spatio-temporal simulation of the novel coronavirus (COVID-19) outbreak using the agent-based modeling approach (case study: Urmia, Iran). *Informatics in Medicine Unlocked*, *20*, Article 100403. https://doi.org/10.1016/j.imu.2020.100403

Harizah, K. (2021, August 27). Highest records to date at 24,599 cases, 393 deaths. *The Malaysian Reserve*. https://themalaysianreserve.com/2021/08/27/highest-records-to-date-at-24599-cases-393-deaths/

Hashim, J. H., Adman, M. A., Hashim, Z., Radi, M. F. M., & Kwan, S. C. (2021). COVID-19 epidemic in Malaysia: Epidemic progression, challenges, and response. *Frontiers in Public Health*, *9*, 1–19. https://doi.org/10.3389/fpubh.2021.560592

Hassan, A. M., Ramos, H., & Moaaz, O. (2023). Second-order dynamic equations with noncanonical operator: Oscillatory behavior. *Fractal and Fractional*, *7*(2), 1–17. https://doi.org/10.3390/fractalfract7020134

He, S., Peng, Y., & Sun, K. (2020). SEIR modeling of the COVID-19 and its dynamics. *Nonlinear Dynamics*, *101*(3), 1667–1680. https://doi.org/10.1007/s11071-020-05743-y

Hinch, R., Probert, W. J. M., Nurtay, A., Kendall, M., Wymant, C., Hall, M., Lythgoe, K., Bulas Cruz, A., Zhao, L., Stewart, A., Ferretti, L., Montero, D., Warren, J., Mather, N., Abueg, M., Wu, N., Legat, O., Bentley, K., Mead, T., … & Fraser, C. (2021). OpenABM-Covid19-An agent-based model for non-pharmaceutical interventions against COVID-19 including contact tracing. *PLoS Computational Biology*, *17*(7), 1–26. https://doi.org/10.1371/journal.pcbi.1009146

Hunter, E., & Kelleher, J. D. (2022). Validating and testing an agent-based model for the spread of COVID-19 in Ireland. *Algorithms*, *15*(08), Article 0270. https://doi.org/10.3390/a15080270

Iderus, N. H., Singh, S., Singh, L., Ghazali, S. M., Ling, C. Y., Vei, T. C., Syahmi, A., Zamri, S., Jaafar, N. A., Ruslan, Q., Huda, N., Jaghfar, A., & Gill, B. S. (2022). Correlation between population density and COVID-19 cases during the third wave in Malaysia: Effect of the Delta Variant. *International Journal of Environmental Research and Public Health, 19*(12), Article 7439. https://doi.org/10.3390/ijerph19127439

Jafar, A., Dollah, R., Sakke, N., Mapa, M. T., Atang, C., Joko, E. P., Sarjono, F., Zakaria, N. S., George, F., & Hung, C. V. (2024). Public perception toward the Malaysian National COVID-19 Immunisation Programme (PICK) in the state of Sabah, Malaysia: A cross-sectional survey. *Disaster Medicine and Public Health Preparedness, 18*, Article e43. https://doi.org/10.1017/dmp.2024.31

Jiee, S. F., Jantim, A., Mohamed, A. F., & Emiral, M. E. (2021). COVID-19 Pandemic: determinants of workplace preventive practice among primary healthcare workers in Sabah, Malaysia. *Journal of Preventive Medicine and Hygiene, 62*(3), Article E605. https://doi.org/10.15167/2421-4248/jpmh2021.62.3.2031

Kim, Y., & Cho, N. (2022). A Simulation study on spread of disease and control measures in closed population using ABM. *Computation*, *10*(01), Article 0002. https://doi.org/10.3390/computation10010002

Kong, L., Duan, M., Shi, J., Hong, J., Chang, Z., & Zhang, Z. (2022). Compartmental structures used in modeling COVID-19: A scoping review. *Infectious Diseases of Poverty*, *11*(1), 1–9. https://doi.org/10.1186/s40249-022-01001-y

Kucharski, A. J., Klepac, P., Conlan, A. J. K., Kissler, S. M., Tang, M. L., Fry, H., Gog, J. R., Edmunds, W. J., Emery, J. C., Medley, G., Munday, J. D., Russell, T. W., Leclerc, Q. J., Diamond, C., Procter, S. R., Gimma, A., Sun, F. Y., Gibbs, H. P., Rosello, A., … & Simons, D. (2020). Effectiveness of isolation, testing, contact tracing, and physical distancing on reducing transmission of SARS-CoV-2 in different settings: A mathematical modelling study. *The Lancet Infectious Diseases*, *20*(10), 1151–1160. https://doi.org/10.1016/S1473-3099(20)30457-6

López, L., & Rodó, X. (2021). A modified SEIR model to predict the COVID-19 outbreak in Spain and Italy: Simulating control scenarios and multi-scale epidemics. *Results in Physics*, *21*, Article 103746. https://doi.org/10.1016/j.rinp.2020.103746

Motzev, M. (2019). Prediction accuracy - A measure of simulation reality. *Vanguard Scientific Instruments in Management*, *15*(1), 1–18. https://doi.org/10.13140/RG.2.2.18743.75687

Mwalili, S., Kimathi, M., Ojiambo, V., Gathungu, D., & Mbogo, R. (2020). SEIR model for COVID-19 dynamics incorporating the environment and social distancing. *BMC Research Notes*, *13*(1), 1–5. https://doi.org/10.1186/s13104-020-05192-1

Nagori, A., Awasthi, R., Joshi, V., Vyalla, S. R., Jarodia, A., Gupta, C., Gulati, A., Bandhey, H., Guliani, K. K., Gill, M. S., Kumaraguru, P., & Sethi, T. (2020). *Less wrong COVID-19 projections with interactive assumptions*. medRxiv. https://doi.org/10.1101/2020.06.06.20124495

Onyechege, D. C., Nor, N. M., & Omer, A. S. F. (2022). The indirect effect of coronavirus disease (COVID-19) pandemic on economic growth in Malaysia: Evidence from the ARDL approach. *International Journal of Economics and Management, 16*(S1), 99-115. https://doi.org/10.47836/ijeamsi.16.1.007

Pandey, G., Chaudhary, P., Gupta, R., & Pal, S. (2019). *SEIR and Regression Model based COVID-19 outbreak predictions in India*. arXiv Preprint.

Patrick, E. M. (2022, January 05). Sabah kesan Omicron pertama [Sabah the first Omicron effect]. *Astro Awani*. https://www.astroawani.com/berita-malaysia/sabah-kesan-kes-omicron-pertama-340088

Paul, S., Mahata, A., Ghosh, U., & Roy, B. (2020). *Since January 2020 Elsevier has created a COVID-19 resource centre with free information in English and Mandarin on the novel coronavirus COVID- 19*. Elsevier.

Qiu, Z., Sun, Y., He, X., Wei, J., Zhou, R., Bai, J., & Du, S. (2022). Application of genetic algorithm combined with improved SEIR model in predicting the epidemic trend of COVID-19, China. *Scientific Reports*, *12*(1), 1–9. https://doi.org/10.1038/s41598-022-12958-z

Qureshi, S., Akanbi, M. A., Shaikh, A. A., Wusu, A. S., Ogunlaran, O. M., Mahmoud, W., & Osman, M. S. (2023). A new adaptive nonlinear numerical method for singular and stiff differential problems. *Alexandria Engineering Journal*, *74*, 585–597. https://doi.org/10.1016/j.aej.2023.05.055

Reeves, K. D., Polk, C. M., Cox, L. A., Fairman, R. T., Hawkins, G. A., Passaretti, C. L., & Sampson, M. M. (2022). Severe acute respiratory coronavirus virus 2 (SARS-CoV-2) infections occurring in healthcare workers after booster vaccination: A comparison of delta versus omicron variants. *Antimicrobial Stewardship and Healthcare Epidemiology*, *2*(1), 1–7. https://doi.org/10.1017/ash.2022.239

Roslan, M. N. F., Ismail, W. I., Zamzuri, A. S., Ismail, N. F., & Abdul, N. A. N. (2022). Comorbidity status of deceased of Covid-19 patients in Malaysia. *International Journal of Academic Research in Business and Social Sciences, 12*(10), 2262-2268. https://doi.org/10.6007/ijarbss/v12-i10/15465

Shah, A. U. M., Safri, S. N. A., Thevadas, R., Noordin, N. K., Rahman, A. A., Sekawi, Z., Ideris, A., & Sultan, M. T. H. (2020). COVID-19 outbreak in Malaysia: Actions taken by the Malaysian government. *International Journal of Infectious Diseases*, *97*, 108–116. https://doi.org/10.1016/j.ijid.2020.05.093

Shamil, S., Farheen, F., Ibtehaz, N., Mahmud, I., & Sohel, K. M. (2021). An agent-based modeling of COVID-19: Validation, analysis, and recommendations. In *Cognitive Computation* (pp. 1723–1734). Springer. https://doi.org/10.1007/s12559-020-09801-w

Silva, P. C. L., Batista, P. V. C., Lima, H. S., Alves, M. A., Guimarães, F. G., & Silva, R. C. P. (2020). COVID-ABS: An agent-based model of COVID-19 epidemic to simulate health and economic effects of social distancing interventions. *Chaos, Solitons and Fractals*, *139*, Article 110088. https://doi.org/10.1016/j.chaos.2020.110088

Tan, C. S., Saim, L., Rao, Y., Kok, S. H., & Ming, L. C. (2021). Public and private sectors collective response to combat COVID-19 in Malaysia. *Journal of Pharmaceutical Policy and Practice, 14*(1), Article 40. https://doi.org/10.1186/s40545-021-00322-x

Tang, X., Zhao, S., Chiu, A. P. Y., Ma, H., Xie, X., Mei, S., Kong, D., Qin, Y., Chen, Z., Wang, X., & He, D. (2017). Modelling the transmission and control strategies of varicella among school children in Shenzhen, China. *PLoS ONE*, *12*(5), 1–17. https://doi.org/10.1371/journal.pone.0177514

Tha, N. O., Shoesmith, W. D., Tan, B. Y., Ibrahim, M. Y., & Hussein, S. S. (2020). Geographic accessibility of healthcare services and health seeking behaviours of rural communities in Kudat and Pitas areas of Sabah. *Borneo Epidemiology Journal, 1*(1), 46-54. https://doi.org/10.51200/bej.v1i1.2436

Thompson, J., & Wattam, S. (2021). Estimating the impact of interventions against COVID-19: From lockdown to vaccination. *PLoS ONE*, *16*, 1–54. https://doi.org/10.1371/journal.pone.0261330

Umair, I. (2022, January 31). The science behind the omicron wave's sharp peak and rapid decline. *The Vox*. https://www.vox.com/22905020/omicron-wave-surge-covid-19-cases-vaccines

World Health Organization. (2023a). *Covid-19*. World Health Organization. https://www.who.int/emergencies/diseases/novel-coronavirus-2019/covid-19-policy-briefs

World Health Organization. (2023b). *WHO Coronavirus (COVID-19) Dashboard*. World Health Organization. https://covid19.who.int/

Yang, Z., Zeng, Z., Wang, K., Wong, S. S., Liang, W., Zanin, M., Liu, P., Cao, X., Gao, Z., Mai, Z., Liang, J., Liu, X., Li, S., Li, Y., Ye, F., Guan, W., Yang, Y., Li, F., Luo, S., … & He, J. (2020). Modified SEIR and AI prediction of the epidemics trend of COVID-19 in China under public health interventions. *Journal of Thoracic Disease*, *12*(3), 165–174. https://doi.org/10.21037/jtd.2020.02.64

Yeo, A. (2020, October 31). Sabah perlu infrastruktur, sistem kesihatan lebih baik [Sabah needs better infrastructure and healthcare systems]. *Berita Harian*. https://www.bharian.com.my/rencana/komentar/2020/10/748301/sabah-perlu-infrastruktur-sistem-kesihatan-lebih-baik

Zhao, W., Sun, Y., Li, Y., & Guan, W. (2022). Prediction of COVID-19 data using hybrid modeling approaches. *Frontiers in Public Health*, *10*, 1–13. https://doi.org/10.3389/fpubh.2022.923978